

Ball-Lens Based Optical Add–Drop Multiplexers: Design and Implementation

Wei Jiang, Yingzhi Sun, Ray T. Chen, *Senior Member, IEEE*, Baoping Guo, James Horwitz, and William Morey

Abstract—Two types of ball-lens based optical add–drop multiplexers (OADMs) are designed and implemented. Insertion losses as low as 0.5 to 0.6 dB for the reflection light-path, and 1.2 to 1.5 dB for the transmission light-path are demonstrated. The 0.5-dB passband is 44% to 50% of the channel spacing and 30% to 33% of –30-dB stopband for 100- and 200-GHz OADMs. The reflection path has an isolation 15 dB. In addition to the distinct cost advantage of ball lenses over the gradient index lenses, the ball-lens based OADMs also offer a significant simplification in packaging. The external diameter of the package is 5.5 mm.

Index Terms—Ball lens, fiber-optic device packaging, GRIN lens, optical add-drop multiplexer (OADM), optical fiber communication, thermally expanded-core (TEC) fiber, thin-film filter, wavelength-division multiplexing.

OPTICAL add–drop multiplexers are indispensable elements in wavelength-division-multiplexed (WDM) networks. Among various approaches to making optical add–drop multiplexers (OADMs), the one utilizing a thin film filter along with a pair of gradient index (GRIN) lenses has taken the lead due to its low cost, satisfactory performance, and high reliability. However, a recent improvement in ball-lens coating technology [1] has enabled ball lenses to offer competitive performance and obvious convenience in packaging, while presenting a distinct cost advantage over GRIN lenses. In this letter, we experimentally demonstrate two designs of ball-lens-based OADMs, whose implementations were demonstrated to have better performance compared to the commercially available GRIN-lens-based counterparts. The intrinsic symmetry of ball lenses also allows a significant simplification in packaging.

In a beam-splitting ball lens proposed earlier [2], a thin-film beam-splitting filter is disposed at the midplane of a full-ball lens. The light is incident on the filter at 45° and is split into two beams traveling perpendicular to each other. However, those narrow-band filters used in OADMs usually have very high transmission loss for large incident angles. Therefore, we design our first OADM (Design A) employing a similar setting, but at nearly normal incidence, as shown in Fig. 1(a). A thin-film filter with a substrate of thickness b and refractive index n_b is sandwiched between two half balls, the filter coating is on the left side. The centers of the fiber endfaces are

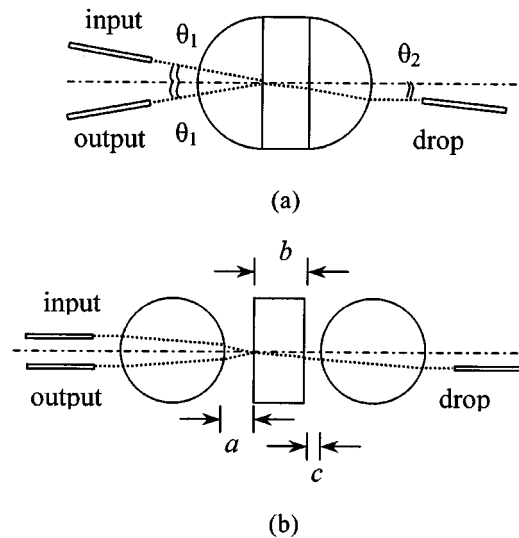


Fig. 1. Optical designs (a) Design A and (b) Design B.

all located on the focal planes of the half balls, with a displacement h from the optical axis. Due to the nonzero thickness of substrate, the drop and output fibers are not symmetric, the two tilting angles are related by

$$\theta_2 = \left[1 - \frac{n_a(n_a - 1)b}{r n_b} \right] \theta_1. \quad (1)$$

where n_a is the refractive index, r the radius of curvature of the half ball. Thermally expanded-core (TEC) fibers are used to reduce the aberration. Detailed calculations based on Seidel aberration [3] and the numerical aperture (NA) versus spot size relation of TEC fibers [4] show that TEC fibers with NA less than 0.08 are required. To reduce cost, we have also considered another design, design B, as shown in Fig. 1(b). It utilizes full-ball lenses to avoid the usage of costly TEC fibers while maintaining low aberration. Full-ball lenses can reduce aberration due to smaller beam radii on lens surfaces compared to half-ball lens. For typical size and glass of the lenses we used, one can show other Seidel aberrations are at least 20 times smaller than the spherical aberration calculated as [3]

$$\text{TSC} = C_1 (u' + i) y i^2 h \quad (2)$$

per surface, where C_1 is a constant, i and u' are incident angle, and after-refraction slope of the marginal ray, y is ray height. One finds the Design B reduces aberration by 8–10 times compared to Design A (assume fiber NA = 0.14). The airgap a is

Manuscript received December 26, 2001; revised February 20, 2002.

W. Jiang, Y. Sun, and R. T. Chen are with the Microelectronics Research Center, University of Texas at Austin, Austin, TX 78758 USA (e-mail: jjiang@ece.utexas.edu).

B. Guo, J. Horwitz, and W. Morey are with the Radiant Photonics, Austin, TX 78758 USA.

Publisher Item Identifier S 1041-1135(02)04359-8.

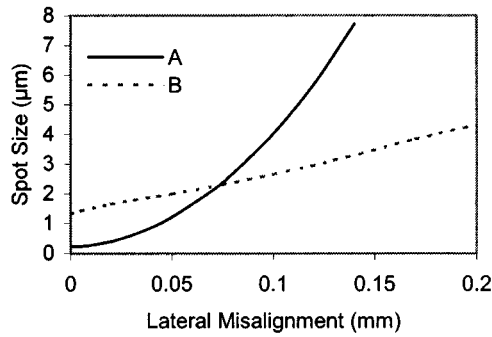


Fig. 2. Spot radius increase due to lateral misalignment between two full/half-ball lens axes for both Designs.

equal to the front focal length of the ball lens, while c is determined by

$$c = a - \frac{b}{n_b}. \quad (3)$$

Fiber endfaces are on the focal planes also. For both designs, detailed calculations find essentially no difference between aberration at the output fibers and drop fibers. The transmission light path is between input and drop fibers, and the reflection light path is between input and output fibers. Note when used as an add multiplexer, the light actually travels from drop fiber to input fiber, and from output fiber to input fiber for these paths.

In implementing these designs, the choice of glass materials and lens radius is subject to the considerations of aberration, packaging size, packaging convenience, cost, and compatibility with filters. We have used lenses with indexes around 1.5 and diameters around 3 mm. The packaging scheme is to first assemble lenses and the filter together into a lens set without alignment. Then the fibers are aligned to the lens set. Aberration analysis for both designs shows that aberration increase is insignificant for typical amounts of lateral misalignments between axes of two lenses (about 0.05 mm, due to mechanical parts holding the lenses), as indicated in Fig. 2. Here, we have used the root-mean-square (rms) spot radius of the image of the input fiber endface center as a measure of aberration. When the spot radius is considerably smaller than the fiber mode-field radius, low insertion loss results. Other misalignments are either equivalent to the lateral misalignment, owing to spherical symmetry, or has a much smaller effect in aberration. For a typical GRIN-lens OADM, there are three alignment steps. They are 1) between a dual-fiber ferrule and one GRIN lens; 2) between a drop fiber ferrule and the other GRIN lens; and (3) between the two GRIN lenses. Our packaging scheme allows us to omit the step 3), where the angular alignment tolerance for GRIN case can be as stringent as 0.05° (for excess loss about 0.5 dB [5]). A packaged ball lens OADM has an outer tube of length 34 mm and diameter 5.5 mm.

Fig. 3(a) shows the spectra of a 200-GHz OADM by Design A, employing two 3.4-mm SF2 lenses and TEC fibers with $NA = 0.04$. The peak insertion losses for reflection path and transmission path are 2.08 and 1.51 dB, respectively. After deducting the reflection loss due to uncoated lenses and TEC fibers, the actual losses are around 1.4 and 0.6 dB,

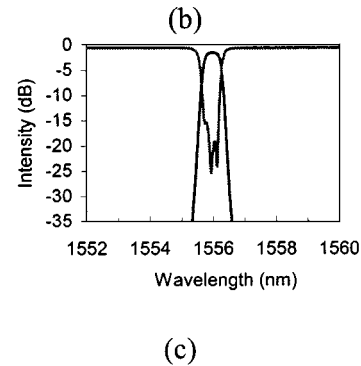
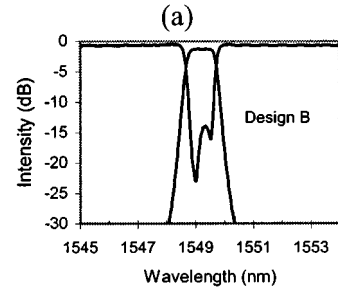
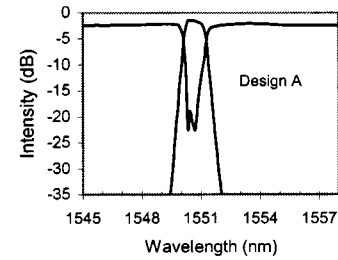


Fig. 3. Spectra of OADM's. (a) 200 GHz, Design A. (b) 200 GHz, Design B. (c) 100 GHz, Design B.

respectively (unless stated explicitly as here, all losses are cited as measured). The high excess loss in reflection path is due to mechanical inaccuracy of tilted v-grooves used to hold the input and output fibers. The 0.5-dB bandwidth (passband) is around 0.71 nm. The isolation for reflection and transmission paths are greater than 15 and 26 dB, respectively. Fig. 3(b) shows the spectra of a 200-GHz OADM by Design B, where 2.5-mm BK7 lenses (antireflection coated) are used. Compared with the original filter data measured at normal incidence (provided by filter manufacturer), the passband decreases from 0.86 to 0.80 nm and -30 -dB stopband increases from 2.24 to 2.41 nm. The central wavelength (CWL) shifts from 1549.63 to 1549.20 nm. The CWL down shift $\Delta\lambda$ is given for small angle of incidence θ by [6]

$$\frac{\Delta\lambda}{\lambda_0} = \frac{\theta^2}{2n^{*2}} \quad (4)$$

where λ_0 is the CWL at normal incidence, and n^* is the effective refractive index. The angle of incidence for Design B is given by

$$\theta = \frac{2h(n_a - 1)}{n_a r} \quad (5)$$

where h is the distance of fibers to the optical axis. According to these formulae, the $\Delta\lambda$ above corresponds to $\theta = 2.15^\circ$, while the designed value is 1.91° , indicating a small angular misalignment of a quarter degree. From this, we can calculate our CWL control accuracy is around 0.09 nm for this type of 200-GHz filter. The transmission path has an insertion loss 1.26 dB. The reflection path has an insertion loss of 0.51 dB and an isolation greater than 16 dB. Shown in Fig. 3(c) are the spectra of a 100-GHz OADM by Design B. The 0.5-dB bandwidth is about 0.35 nm. The insertion losses are 0.54 and 1.44 dB for reflection and transmission paths, respectively. The -30 -dB stopband width is 1.15 nm for the transmission path. The isolation of reflection path is better than 15 dB. Overall, these values of insertion losses, bandwidths, and isolations are better than the typical specifications of GRIN lens OADMs [7]. Ripple and polarization-dependent loss are generally less than 0.25 dB.

Generally, our experiments show that in Design A, the lenses and the filter are easily packaged together. But TEC fibers are required for this design. For Design B, to separate the lenses and filter at certain spacing adds to the complexity of the packaging, but low aberration is achieved without TEC fibers.

In summary, we have designed and implemented two types of ball-lens based OADMs. Design A has a packaging advantage,

but needs TEC fibers, while Design B uses standard fibers. The performance of ball-lens OADMs is competitive compared to GRIN lens OADMs. The simplification in alignment and the cost advantage makes ball-lens OADMs more attractive.

ACKNOWLEDGMENT

The authors would like to thank Dr. F. Zhao, Dr. J. Qiao, Dr. X. Deng, and C. Yang for many helpful discussions, and to R. Collins for lab assistance.

REFERENCES

- [1] T. Clark and K. Wanser, "Ball vs. gradient index lenses," *Photonics Spectra*, pp. 94–96, Feb. 2001.
- [2] J. Ai, J. Popelek, Y. Li, and R. T. Chen, "Beam-splitting ball lens: A new integrated optical component," *Opt. Lett.*, vol. 24, pp. 1478–1480, 1999.
- [3] W. J. Smith, *Modern Optical Engineering*. New York: McGraw-Hill, 2000, pp. 301–366.
- [4] K. Shiraishi, Y. Aizawa, and S. Kawakami, "Beam expanding fiber using thermal diffusion of the dopant," *J. Lightwave Technol.*, vol. 8, pp. 1151–1161, Aug. 1990.
- [5] S. Yuan and N. A. Riza, "General formula for coupling-loss characterization of single-mode fiber collimators by use of GRIN rod lenses," *Appl. Opt.*, vol. 38, pp. 3214–3222, 1999.
- [6] H. A. Macleod, *Thin-Film Optical Filters*, 2nd ed. New York: McGraw-Hill, 1989.
- [7] "OADM 101A/D Series Specifications Sheet," Oplink Communications, Inc., 2001.